Proc. Natl. Acad. Sci. USA
Vol. 86, pp. 9822–9826, December 1989
Biophysics

Three-dimensional ordered distribution of crystals in turkey tendon collagen fibers

WOLFIE TRAUB*, TALMON ARAD*, AND STEPHEN WEINER†

*Structural Chemistry and †Isotope Departments, Weizmann Institute of Science, Rehovot 76100, Israel

Communicated by H. A. Scheraga, July 31, 1989

ABSTRACT **The organization of apatite crystals and collagen fibrils in mineralized turkey tendon has been studied by electron microscopy and electron diffraction. To minimize artifactual distortions the tissue was examined, for the first time, as isolated fibrils in an aqueous environment of vitreous ice, as well as in conventionally prepared sections. The electron micrographs show that the plate-shaped apatite crystals are arranged in parallel arrays across the collagen fibrils. This provides direct evidence for highly asymmetric assembly in collagen fibrils, and, indeed, the fibrils were observed to be elongated rather than round in cross-section. There is, furthermore, a pronounced tendency for the layers of crystals to be coherently aligned in adjacent fibrils. These observations may also be important for understanding the mechanical behavior of bone at the molecular level, as such extended, aligned aggregates of flat crystals could develop into natural fracture planes in mature bone.**

The structure and mechanical properities of bone derive, at the molecular level, from the organized growth of carbonated calcium phosphate (apatite) crystals within a matrix of collagen fibrils and other organic components (1). Newly formed bone has a relatively low mineral content, consisting of small crystals closely associated with the collagen fibrils, whereas in denser more mature bone many crystals are larger and not obviously related to the collagen structure. Although the early formed crystals have been shown to grow with preferred orientation in gap regions between collagen molecules (2–4), much remains to be understood about the shape, orientation, and distribution of crystals within the organic matrix, as well as the factors that initiate and control their growth. We have investigated crystal distribution in mineralized turkey tendon, a tissue often regarded as a model for some portions of bone (5–10), in which almost all the mineral crystals are associated with parallel collagen fibrils. This arrangement would therefore approximate most closely to newly formed bone.

Several unusual experimental procedures have been used in our studies of turkey tendon. (*i*) By using ultrasonication we have been able to isolate intact single fibrils of mineralized collagen in which the very thin plate-like apatite crystals are generally much better visualized than in more conventional preparations of embedded sections. (*ii*) These fibrils have been studied in an aqueous environment of vitreous ice, thus avoiding the dehydration and consequent distortion of unprotected fibrils in the high vacuum of the electron microscope. (*iii*) We have determined the orientations and relative alignment of apatite crystals over extensive regions of the tendon by examining critical features in their electron diffraction patterns. These experiments have provided insights into the assembly structure of this much-studied tissue, which our results show to be remarkably regularly organized. We have recently obtained some evidence that similar regular structures also exist in bone and may explain some of its mechanical properties.

The publication costs of this article were defrayed in part by page charge payment. This article must therefore be hereby marked "*advertisement*" in accordance with 18 U.S.C. §1734 solely to indicate this fact.

MATERIALS AND METHODS

Thin elongated mineralized leg tendons from freshly sacrificed 21-week-old domestic turkeys were kept frozen until use, then cleaned of adhering tissue and nonmineralized collagen, and dissected. Pieces (≈1 mm) were plunged into liquid nitrogen and then crushed in a precooled agate mortar and pestle. The powder was suspended in ≈0.25 ml of deionized water and sonicated (Branson ultrasonic cleaner, 1.0 A) for 15–30 min to a milky white suspension. A drop was placed on a 300-mesh grid with a support film of pioloform reinforced with a thin layer of carbon, left for 3 min, then blotted, and rapidly plunged (11) into liquid ethane to produce vitrification (12). The samples were transferred under liquid nitrogen to the electron microscope by using a Gatan (Pleasanton, CA) cryotransfer system and specimen holder. Other portions of flat mineralized tendons were embedded in Epon and sectioned parallel (longitudinally) as well as perpendicular (transverse) to the flat natural surface. The specimens were examined in image and diffraction modes in a Philips 400T transmission electron microscope.

RESULTS

Many of the fibrils we have observed (Figs. 1–4) show banding patterns corresponding to the well-known 64-nm collagen periodicity. As no stain was applied to the specimens, the higher density is evidently due to the preferential presence of mineral crystals in the gap zone (2–4).

Fig. 1 shows a turkey tendon fiber splayed out into some ten separated fibrils about 50 nm in diameter. There are also many separated apatite crystals in various orientations. Those lying flat appear as somewhat irregular elongated plates of rather low density. Those seen edge-on appear much denser and look needle-like. That these are different views of similar objects can be seen by examining different regions of the fibrils. In low-density regions (Fig. 1A) where crystals lie mainly flat, the banding pattern is seen clearly, indicating that crystals lie predominantly in the collagen gap region. Where crystals are seen mostly edge-on (e.g., Fig. 1*B*), they appear denser, and it is difficult to see the banding. A single twisted fibril (Fig. 1*C*) can show both views.

A twisted fibril at higher magnification (Fig. 2) shows appreciable dimensional asymmetry, with the fibril width 150 nm in the plane of the crystals (Fig. 2*A*) and the width only ≈75 nm looking at the crystals edge-on. We have been able to tilt such speciments by angles to 50° in the electron microscope and see portions of the fibrils and even individual crystals interchanging between flat and edge-on views. The edge-on view (Fig. 2*B*) also shows that the crystal planes are nearly parallel to each other and to the long axis of the collagen fibril. Electron diffraction patterns (see below) show that the crystallographic *c* axes of the apatite crystals are lined up along this direction.

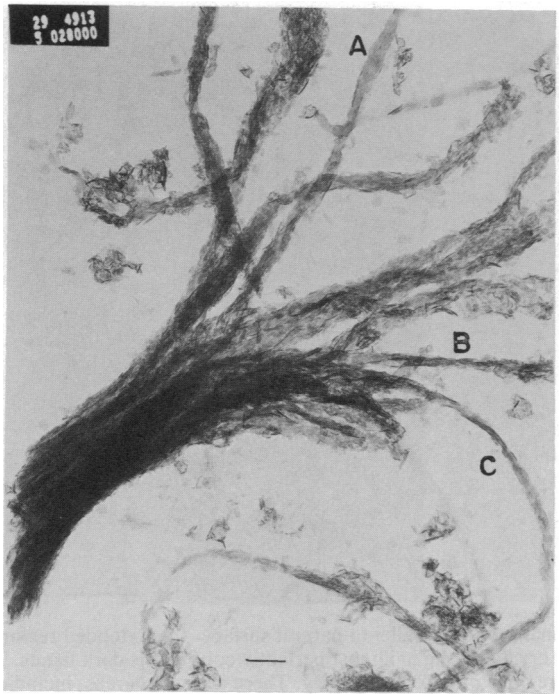

FIG. 1. Electron micrograph of vitreous ice preparation of mineralized turkey tendon fiber composed of several fibrils. Different regions show apatite crystals lying mainly flat (*A*) and mainly edge-on (*B*), sometimes in the same fibril (*C*). (Bar = 0.2 μm.)

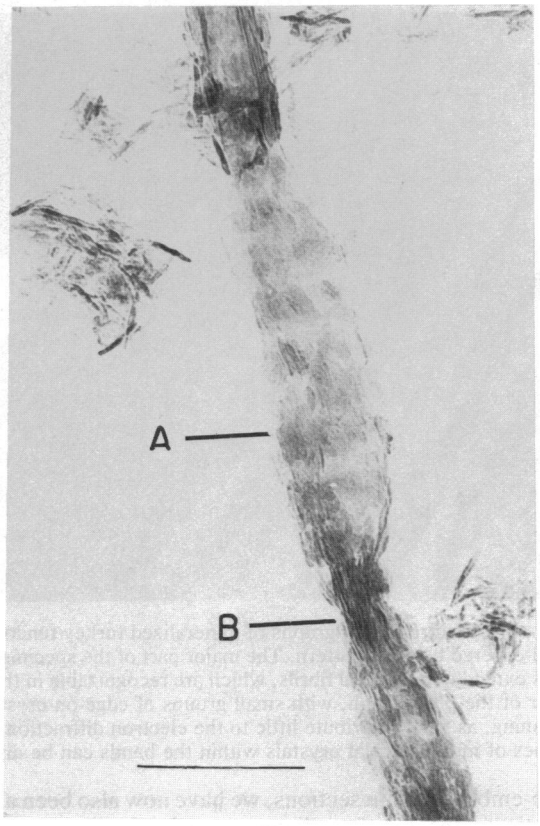

FIG. 2. Twisted mineralized turkey tendon fibril in vitreous ice showing different widths viewed perpendicular (*A*) or parallel (*B*) to planes of the cystals. (Bar = 0.2 μm.)

We have confirmed that these specimens really are embedded in vitreous ice by observing its characteristic diffraction pattern in regions adjacent to the fibrils. However, the most dramatic demonstration is the great sense of depth evident in stereo views of these preparations. In Fig. 3 the different heights of various structural features in the vitreous ice can be seen particularly well in the bottom left portion. More significantly, the stereo allows one to see several layers of flat crystals stacked on top of each other as one looks through the main fibril. The lengths of the crystals along the fibril appear somewhat more than half a banding period, suggesting that crystals may be growing out of the gaps into the overlap zones.

These results from vitreous ice preparations confirm and extend our earlier report (8) concerning the ordered stacking of plate-like apatite crystals within dehydrated collagen fibrils. The vitrification does not appear to have affected the shapes and sizes of the crystals. With the aid of well-oriented

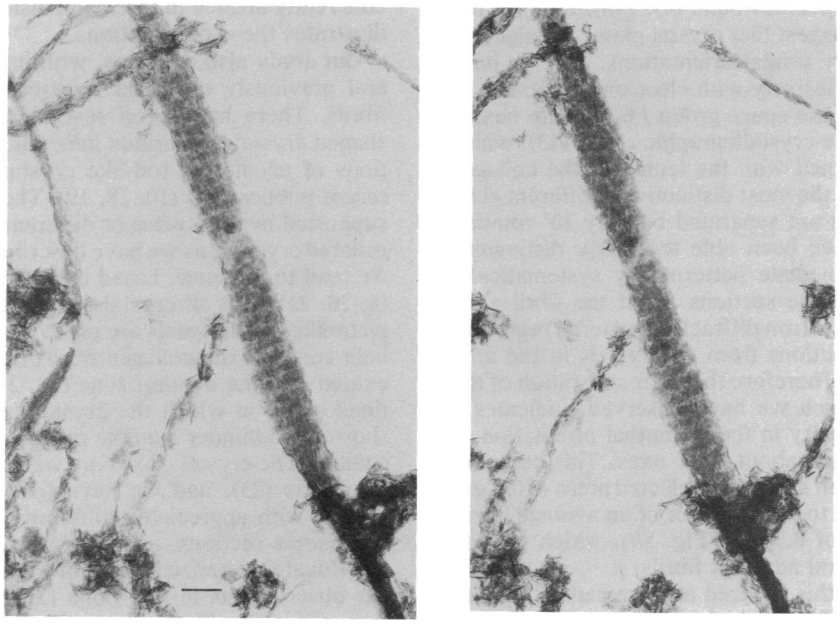

FIG. 3. Stereo view of mineralized turkey tendon in vitreous ice. Note depth of view in bottom left portion and stacked layers of crystals in main fibril. (Bar = 0.2 μm.)

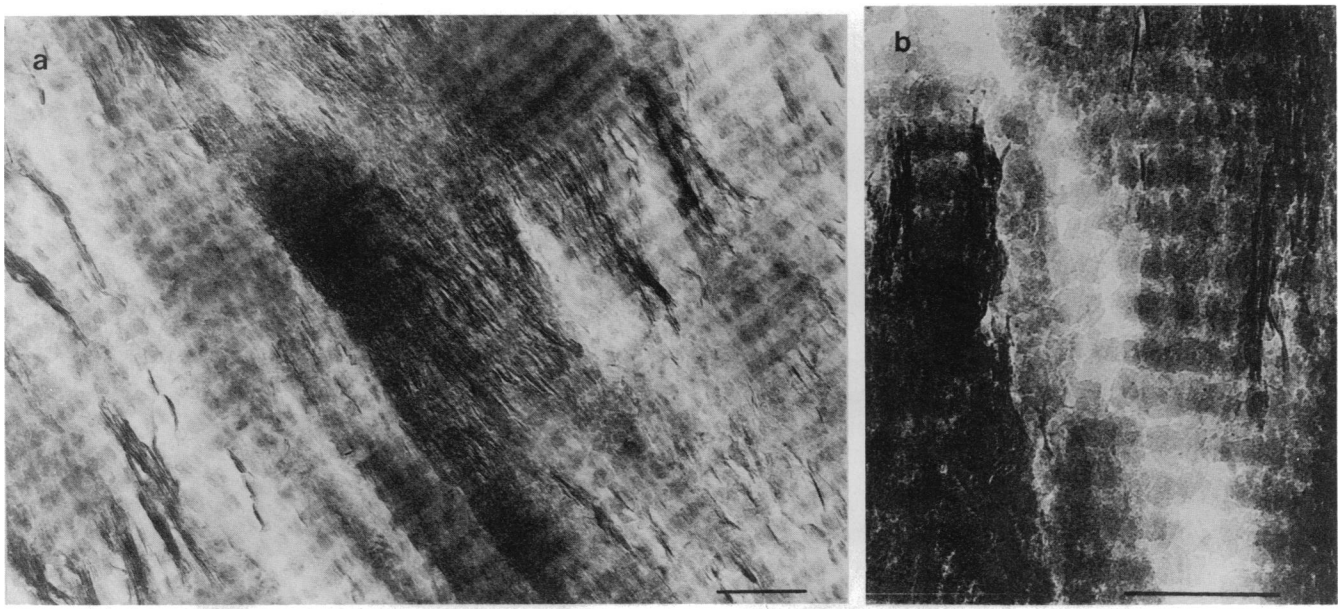

FIG. 4. Electron micrographs of mineralized turkey tendon cut in longitudinal section parallel to natural surface. (*a*) Extended region with a well-ordered banding pattern. The major part of the specimen consists of flat crystals lying in almost perfectly continuous dark bands. These bands extend over several fibrils, which are recognizable in the micrograph as regions of different density. There are a few areas, including the center of the photograph, with small groups of edge-on crystals that appear needle-like. These are probably superficial disorders caused by sectioning, as they contribute little to the electron diffraction pattern. (cf. Fig. 5*b*). (*b*) A thin section near the junction of two fibrils in which outlines of individual flat crystals within the bands can be discerned. (Bars = 0.2 μm.)

Epon-embedded thin sections, we have now also been able to investigate the relative alignments of crystals in adjacent fibrils.

Fig. 4 shows longitudinal sections in which flat crystals are arranged in remarkably well-ordered banding patterns that extend over several individual fibrils. In some regions, near the edges of adjacent fibrils, individual crystals can be discerned (Fig. 4*b*). Such areas show that the lengths of the crystals along the fibril axis are generally somewhat greater than half the banding period, but that the widths along the bands are less well defined, although generally smaller than the lengths. The axial lengths of adjacent fibrils in Fig. 4 are well aligned, and the gap regions, in which the crystals are mainly located, are almost everywhere in register longitudinally, as has also been seen in bone (4). Furthermore, our electron micrographs suggest that crystal plates in neighboring fibrils may have very similar orientations. This we have been able to show conclusively with electron diffraction.

Apatite crystals have the space group $P6_3/m$ with hexagonal symmetry about the crystallographic *c* axis (13), which in turkey tendon is aligned with the length of the collagen fibril (5). Consequently, the most distinctively different electron diffraction patterns are separated by only 30° rotation about this axis. We have been able to clearly distinguish these, as well as intermediate patterns, by systematically tilting selected areas of the sections about the fibril axial direction (Fig. 5). The electron diffraction patterns represent a summation of contributions from all crystals in the area selected for diffraction. Therefore the clear separation of the diffraction patterns, which we have observed, indicates a high degree of homogeneity in the azimuthal orientation of the crystals—i.e., rotation about the *c* axes. This coherent crystal alignment has been shown for selected areas of 0.3 μm (Fig. 5*a*), corresponding to the diameter of an average fibril, and also for the areas of 0.9 μm (Fig. 5*b*), which include contributions from several adjacent fibrils.

Further evidence for this ordered arrangement of apatite crystals is presented in Fig. 6, which shows a stereo view of a nearly transverse section of adjacent fibrils. The plate-like crystals are seen mainly end-on (in the left portion of the fibrils) and look like needles, which are seen to run parallel from one fibril to the next. However, the side view of the fibrils (on right) shows that these "needles" correspond to the edges of stacked parallel layers of plate-like crystals. The crystals are present throughout the fibrils, not just on the periphery, as has been reported for younger tendon (10).

DISCUSSION

This study confirms, with specimens in vitreous ice, an earlier observation (8) that the distinctive bands across the collagen fibrils in mineralized turkey tendon are composed of several parallel layers of coplanar plate-shaped crystals. It also shows that the mineralized fibrils are not cylindrically symmetrical and that crystals in adjacent fibrils tend to be coherently aligned in three dimensions. Fig. 7 schematically illustrates these observations.

Our study also confirms, with improved techniques, several previously observed features of mineralized collagen fibrils. There have been several reports (14–17) of plate-shaped crystals in various mineralized tissues; yet, descriptions of needle- or rod-like crystals persist, even in very recent publications (10, 18, 19). These latter reports are not supported by transverse or different tilted views of fibers or isolated crystals, as we have described above. Until they are, we tend to the view, based on quite extensive observations (8, 20, 21), that all crystals in turkey tendon and bone are plate-like. The crystals are preferentially associated with the hole zones of the collagen fibrils (22), but some at least do extend into the overlap zone (10, 21). Presumably the confined space in which the crystals grow makes them much shorter and thinner than the rod-like apatite crystals of tooth enamel. The crystal *c* axes are well aligned with the collagen fibril axis (23), and we have found no evidence of fibril regions with appreciably different crystal orientations (10). Transverse sections, as well as stereo longitudinal views of individual mineralized fibrils of mature tendon, support earlier observations in fish bone (3) that crystals are located throughout the fibrils. In contrast, transverse sections of early mineralized turkey tendon (10) and embryonic fish dentin (19) show no crystals located in the fibril cores. These

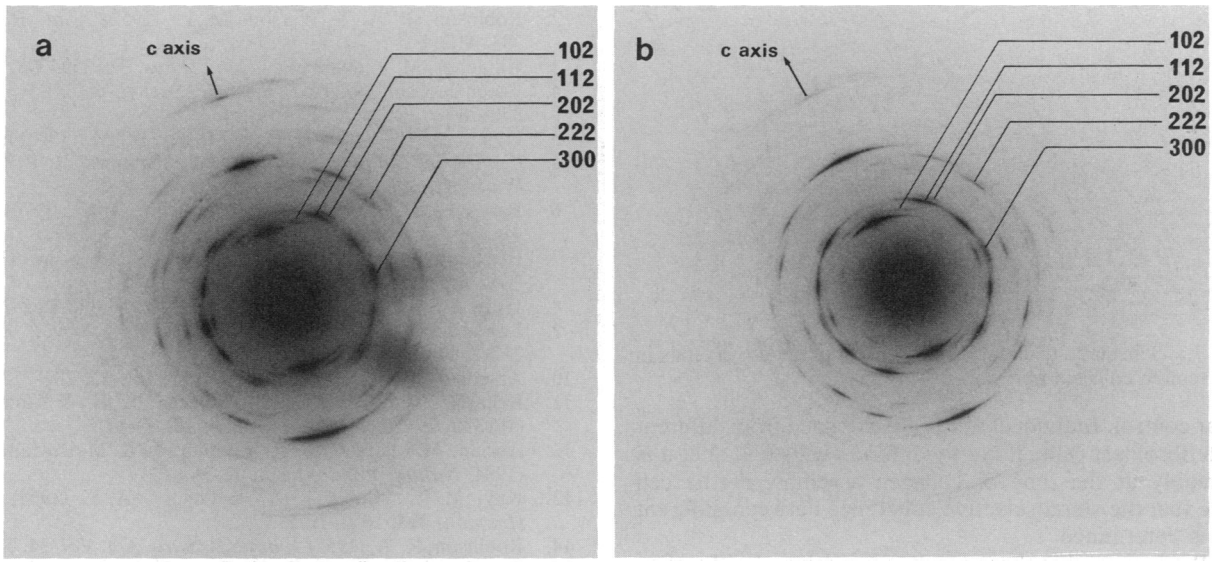

FIG. 5. Electron diffraction patterns of longtudinal sections of mineralized turkey tendon. (*a*) Diffraction from selected area of 0.3-μm diameter. This pattern shows *h o l*-type reflections (e.g., 300, 102, and 202) relatively intense compared with *h h l*-type reflections (e.g. 112, 222), in contrast to that of *b*, indicating well-defined orientation of apatite crystallites with their *b* axes lined up with the electron beam. (*b*) Diffraction from selected area of 0.9-μm diameter, corresponding to most of the region shown in Fig. 4*a*. This pattern shows *h h l*-type reflections, including 112 and 222, relatively intense compared with *h o l*-type reflections, such as 300, 102, and 202. This indicates a nearly uniform orientation of the crystallites with their 100 faces perpendicular to the electron beam and tilted some 30° about their *c*-axis directions from the orientation of Fig. 5*a*. Some distortions were evidently introduced into the specimens during sample preparation, so the best areas were sought. As shown here, well-oriented and balanced diffraction patterns corresponded to well-ordered banding patterns in electron micrographs. However, diffraction proved the more sensitive criterion, so regions for data collection were sought first in the "image" and then in the "diffraction" mode of the electron microscope.

different observations suggest that mineralization starts at the periphery of the fibrils and proceeds inwards (5).

Our structural findings also have several significant wider implications. (*i*) The observed arrangement of plate-like crystals in parallel arrays within the fibrils provides information on the structure of collagen itself. It has been proposed that the crystals are located in parallel grooves (8) that are at least one order of magnitude wider than the gaps between the ends of individual collagen molecules (24). These grooves could result from the lining up of adjacent gaps as proposed in some (25, 26) of the many models for collagen assembly. Further experimental support for the existence of grooves even in unmineralized collagen fibrils comes from image-enhanced cross-sectional views of rat tail tendon (27) and the locations and stoichiometry of the cross-links in collagen from periodontal ligament (28). Note too that the observation of the same equatorial diffraction spacing in dried mineralized and unmineralized tissue (6, 19) is consistent with the presence of crystals in grooves separated by four rows of collagen molecules.

(*ii*) The longitudinal and azimuthal alignment of crystals in adjacent collagen fibrils indicates a remarkable degree of

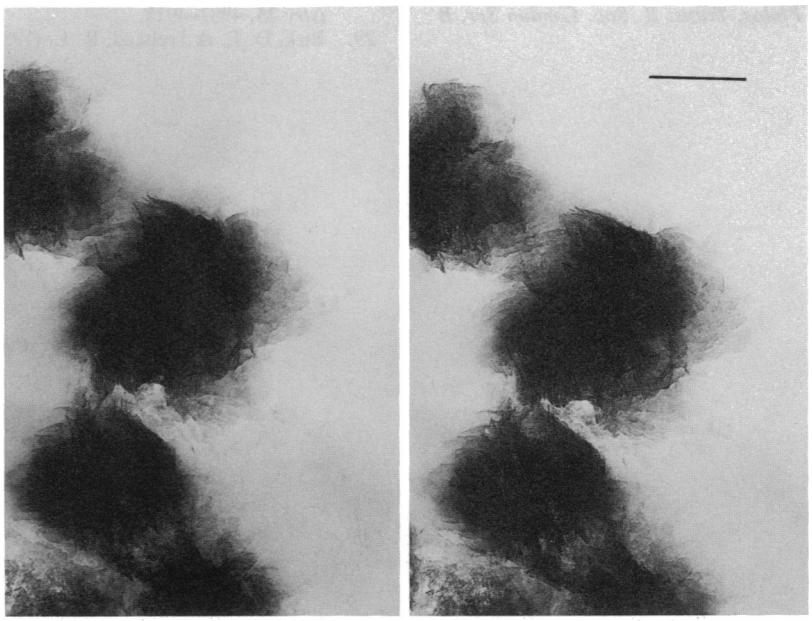

FIG. 6. Stereo view of an almost transverse section of mineralized turkey tendon fibrils, showing how the flat crystals are arranged in layers. (Bar = 0.2 μm.)

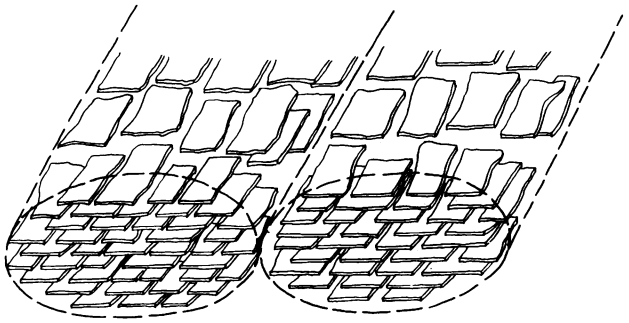

FIG. 7. Schematic diagram of distribution of apatite crystals in turkey tendon collagen fibrils.

cellular control. Individual fibrils are extruded from different loci on fibroblast cells, if not by different cells (29). Yet it is presumably at the time of collagen assembly at the cell surface that the stereoselective coherence between different fibrils is determined.

(*iii*) We believe that these results from mineralized turkey tendon may have relevance to some of the more complex ultrastructures found in bone. Bones also have plate-like crystals, some of which are much larger than those found in turkey tendon (20). Transmission electron microscope micrographs of embedded and sectioned bone are generally consistent with parallel arrays of crystals within fibrils (seen usually only edge-on), except for crystals in matrix vesicles (9, 10). Furthermore, scanning electron microscope studies of heavily mineralized mammalian bones show surface fractures that are smooth and stepped, with indications of preferred fibril orientation, whereas less mineralized bones show rounded fibrous fractures (21). We suggest that further crystal growth in the kind of organized structure we have observed in turkey tendon could lead to extended planar crystalline aggregates along which bones would naturally fracture.

We are grateful to Victor Benghiat, Sam Gordon, and Stanley Himmelhoch for their help in sample preparations and to Shmuel Hurwitz, Faculty of Agriculture, Hebrew University, for providing the turkey. This study was supported by grants from the U.S. Public Health Service (DEO6954) and the Minerva Foundation.

1. Glimcher, M. J. (1984) *Philos. Trans. R. Soc. London Ser. B* **304,** 479–508.
2. Robinson, R. A. & Watson, M. L. (1952) *Anat. Rec.* **114,** 383–410.
3. Glimcher, M. J. (1959) *Rev. Mod. Phys.* **31,** 359–393.
4. Fitton Jackson, S. (1957) *Proc. R. Soc. (London) Ser. B* **146,** 270–280.
5. Nylen, M. U., Scott, D. B. & Mosley, V. M. (1960) in *Calcification in Biological Systems*, ed. Sognnaes, R. F. (AAAS, Washington, DC), pp. 129–142.
6. Eanes, E. D., Lundy, D. R. & Martin, G. N. (1970) *Calcif. Tissue Res.* **6,** 239–248.
7. Berthet-Colominas, C., Miller, A. & White, S. W. (1979) *J. Mol. Biol.* **134,** 431–445.
8. Weiner, S. & Traub, W. (1986) *FEBS Lett.* **206,** 262–266.
9. Landis, W. J. (1986) *J. Ultrastruct. Mol. Struct. Res.* **94,** 217–238.
10. Arsenault, L. A. (1988) *Calcif. Tissue Int.* **43,** 202–212.
11. Bellare, J. R., Davis, H. T., Scriven, L. E. & Talmon, Y. (1988) *J. Electron Microsc. Tech.* **10,** 87–111.
12. Adrian, M., Dubochet, J., Lepault, J. & McDowall, A. W. (1984) *Nature (London)* **308,** 32–36.
13. Kay, M. I., Young, R. A. & Posner, A. S. (1964) *Nature (London)* **204,** 1050–1052.
14. Robinson, R. A. (1952) *J. Bone Jt. Surg. Am. Vol.* **34,** 389–434.
15. Termine, J. D., Eanes, E. D., Greenfield, D. J., Nylen, M. U. & Harper, R. A. (1973) *Calcif. Tissue Res.* **12,** 73–90.
16. Johansen, D. M. D. & Parks, H. F. (1960) *J. Biophys. Biochem. Cytol.* **7,** 743–745.
17. Jackson, S. A., Cartwright, A. G. & Lewis, D. (1978) *Calcif. Tissue Res.* **25,** 217–222.
18. Bigi, A., Ripamonti, A., Koch, M. H. J. & Roveri, N. (1988) *Int. J. Biol. Macromol.* **10,** 282–286.
19. Lees, S. & Prostak, K. (1988) *Connect. Tissue Res.* **18,** 41–54.
20. Weiner, S. & Price, P. A. (1986) *Calcif. Tissue Int.* **39,** 365–375.
21. Weiner, S. & Traub, W. (1989) in *Proceedings of 3rd International Conference on the Chemistry and Biology of Mineralized Tissues*, ed. Glimcher, M. J. (Gordon & Breach, New York), in press.
22. Hodge, A. J. & Petruska, J. A. (1963) in *Aspects of Protein Structure*, ed. Ramachandran, G. N. (Academic, New York), pp. 289–300.
23. Schmidt, W. J. (1936) *Naturwissenschaften* **24,** 361.
24. Bornstein, P. & Traub, W. (1979) in *The Proteins*, eds. Neurath, H. & Hill, R. L. (Academic, New York), Vol. 4, pp. 411–632.
25. Katz, E. P. & Li, S. (1973) *J. Mol. Biol.* **73,** 351–369.
26. Fraser, R. D. B., MacRae, T. P., Miller, A. & Suzuki, E. (1983) *J. Mol. Biol.* **167,** 497–521.
27. Hulmes, D. J. S., Holmes, D. F. & Cummings, C. (1985) *J. Mol. Biol.* **184,** 473–477.
28. Yamauchi, M., Katz, E. P. & Mechanic, G. L. (1986) *Biochemistry* **25,** 4907–4913.
29. Birk, D. E. & Trelstad, R. L. (1986) *J. Cell Biol.* **103,** 231–240.